

Numerical modelling of the damaging behaviour of the reinforced concrete structures by multi-layers beams elements

Khebizi Mourad* and Guenfoud mohamed

Department of Civil Engineering, University of Guelma, LP 401 Guelma, Algeria

(Received February 20, 2014, Revised January 18, 2015, Accepted January 27, 2015)

Abstract. A two-dimensional multi-layered finite elements modeling of reinforced concrete structures at non-linear behaviour under monotonic and cyclical loading is presented. The non-linearity material is characterized by several phenomena such as: the physical non-linearity of the concrete and steels materials, the behaviour of cracked concrete and the interaction effect between materials represented by the post-cracking filled. These parameters are taken into consideration in this paper to examine the response of the reinforced concrete structures at the non-linear behaviour. Four examples of application are presented. The numerical results obtained, are in a very good agreement with available experimental data and other numerical models of the literature.

Keywords: modelling; multi-layers finite elements; damage; non-linear behaviour; unilateral model

1. Introduction

The non-linear behaviour modelling of reinforced concrete structures is an important objective for the civil engineering researchers. The response of a structure under a loading results from a strong interaction between the materials effects (local non-linearity), the structures effects (geometry, distribution of forces and stiffness, links) and the environment effect (soil-structure interaction). The local non-linearities are related particularly to the formation, the opening and reclosure of cracks, on one hand, to the link and to the behaviour of the reinforcements (plasticity of steels) on the other hand. A good description of these phenomena has to be done in order to represent the variations of the structural stiffness and to have access to the behavior until to the collapse.

In this paper we have presented a numerical method for modelling planar reinforced concrete structure (2D) under static and cyclical loading. This method uses multi-layered beams elements of which the stiffness matrix is computed using a beam discretization according to the height in superimposed successive layers (Fig. 1). The summation of these layers allows the calculation of stiffness in a correct manner and takes into account the behaviour variations. The Bernoulli hypothesis (section remaining plane and perpendicular to the neutral axis of the beam) confers for

*Corresponding author, Assistant Professor, E-mail: Mourad_gc@yahoo.fr

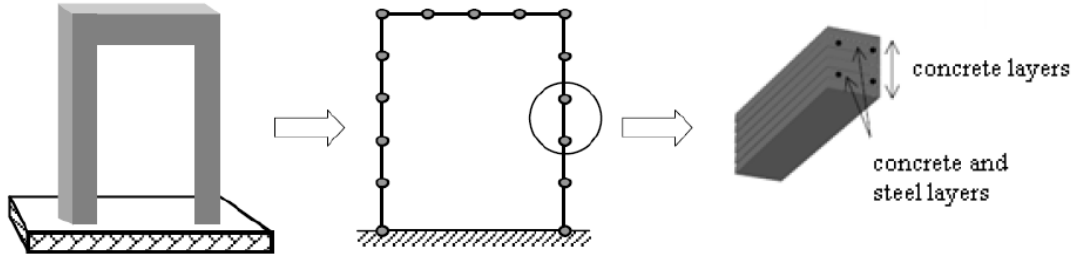


Fig. 1 Discretisation principal of reinforced concrete structures with multi-layered beam

different layers a uniaxial behaviour. Hence, this allows as to treat the local behaviours through uniaxial laws for the concrete and steel, laws that are assigned to each layer. The calculation of inelastic efforts is carried through to an iteration method based on the initial secant stiffness.

A particular treatment is reserved for the layers including simultaneously concrete and steel. The behaviour of the mixed layers (Fig. 1) is homogenized by a mixing law permitting to calculate the stress layer in proportion to each material:

$$\sigma_{layer} = (1 - A)\sigma_{concrete} + A\sigma_{steel} \quad (1)$$

where σ_{layer} denote axial stresses in the layer, $\sigma_{concrete}$ and σ_{steel} axial stresses in the concrete and the steel respectively in the layer and A is the relative area of steel within the reinforced layer. The steel-concrete adherence is supposed to be perfect (identical strain of the two materials at their frontier: $\varepsilon_{concrete} = \varepsilon_{steel}$).

2. Formulation of multi-layered beam element

The elements used are beams with tow nodes, the Bernoulli hypothesis confers on the various layers a uniaxial behaviour. The relation giving the element equilibrium is obtained by the virtual work principle, expressed in terms of generalized coordinates.

$$\delta U^T F = \int_{\Omega} \delta \varepsilon^T \sigma dV \quad (2)$$

with

$$\delta \varepsilon^T = \delta (BU)^T = \delta U^T B^T \quad (3)$$

where B : depends on the derived shape functions

If can be introduced a behaviour law with damage and anelastic,

$$\varepsilon = \frac{\sigma}{E(1-D)} + \varepsilon_{an}(D) \quad (4)$$

or

$$\sigma = E(1-D)(\varepsilon - \varepsilon_{an}) \quad (5)$$

The virtual work principle takes the following form:

$$\delta U^T F = \int_{\Omega} \delta U^T B^T E(1-D)(\varepsilon - \varepsilon_{an}) \quad (6)$$

or,

$$F = \int_{\Omega} B^T E(1-D)(\varepsilon - \varepsilon_{an}) dV \quad (7)$$

Eq. (7) can be rewritten in the following form:

$$F = \left[\int_{\Omega} B^T E(1-D) B dV \right] U - \int_{\Omega} B^T E(1-D) \varepsilon_{an} dV \quad (8)$$

By putting:

$$K = \int_{\Omega} B^T E(1-D) B dV \quad (9)$$

and

$$F_{an} = - \int_{\Omega} B^T E(1-D) \varepsilon_{an} dV \quad (10)$$

We end up with the final system to solve:

$$F = KU + F_{an} \quad (11)$$

K is the element stiffness matrix:

$$K = \int_0^l B^T k_s B dx \quad (12)$$

The section stiffness matrix is expressed as follows:

$$k_s = \begin{bmatrix} k_{11} & k_{12} \\ k_{21} & k_{22} \end{bmatrix} \quad (13)$$

with

$$k_{11} = \int_s E ds \quad k_{12} = k_{21} = \int_s E y ds \quad k_{22} = \int_s E y^2 ds \quad (14)$$

The discretization of the cross-section in superimposed layers according to the Bernoulli hypothesis allows to be obtaining the following stiffnesses (Belmouden 2004):

$$k_{11} = \sum_{k=1}^{nlayers} E_k A_k \quad k_{12} = k_{21} = \sum_{k=1}^{nlayers} E_k y_k A_k \quad k_{22} = \sum_{k=1}^{nlayers} E_k y_k^2 A_k \quad (15)$$

E_k , A_k and y_k are respectively the Young modulus, the layer area and the centre position layer to the reference axis.

3. Damage model for the concrete (Unilateral model)

The unilateral model (Laborderie 1991, Kotronis 2000, Davenne et al. 2003) is an isotropic model where two scalar damage variables, are used to describe the consequences of the evolution of the mechanical characteristics of material, the irreversible strains and the unilateral effect when the sign of the stresses changes. Considering the partition of the strain tensor as the sum of an elastic part and an anelastic part, calculated as follows:

$$\varepsilon = \varepsilon_e + \varepsilon_{an} \quad (16)$$

$$\varepsilon_e = \frac{\sigma^+}{E_0(1-D_1)} + \frac{\sigma^-}{E_0(1-D_2)} + \frac{\nu}{E_0} (\sigma - (Tr\sigma)I) \quad (17)$$

$$\varepsilon_{an} = \frac{\beta_1 D_1}{E_0(1-D_1)} \frac{\partial f(\sigma)}{\partial \sigma} + \frac{\beta_2 D_{21}}{E_0(1-D_2)} I \quad (18)$$

where: E_0 is the initial Young modulus and ν the Poisson ratio. σ^+ denotes the positive part of a tensor, D_1 and D_2 are scalar damage variable in tension and scalar damage variable in compression respectively (their evolution between 0 – i.e, healthy material- to 1 - i.e, broken material- is related to the local elastic energy), β_1 et β_2 are material parameters to be identified in order to describe the evolution of the anelastic strains can be described, $f(\sigma)$ is the crack closure function which cancels the anelastic strains of the tension during the recovery of stiffness and σ_f the crack closure stress :

$$Tr(\sigma) \in [0, +\infty[\rightarrow \frac{\partial f(\sigma)}{\partial \sigma} = 1 \quad (19)$$

$$Tr(\sigma) \in [-\sigma_f, 0[\rightarrow \frac{\partial f(\sigma)}{\partial \sigma} = \left(1 + \frac{Tr(\sigma)}{\sigma_f} \right) = 1 \quad (20)$$

$$Tr(\sigma) \in [-\infty, -\sigma_f[\rightarrow f(\sigma) = 0.1 \quad (21)$$

The evolution laws for the damage are finally written as:

$$D_i = 1 - \frac{1}{1 + (A_i(Y_i - Y_{0i}))^{B_i}} \quad (22)$$

with Y_i is the variable associated to damage (energy refund ratio, tension or compression).

A_i and B_i are material constants.

Y_{0i} is the damage threshold (tension or compression).

The stress-strain relationship and the crack closure function in the uniaxial model can be written as follows:

$$\varepsilon = \frac{\sigma^+}{E_0(1-D_1)} + \frac{\sigma^-}{E_0(1-D_2)} + \frac{\beta_1 D_1}{E_0(1-D_1)} F(\sigma) + \frac{\beta_2 D_2}{E_0(1-D_2)} \quad (23)$$

$$F(\sigma) = 1 \quad si \quad \sigma \geq 0 \quad (24)$$

$$F(\sigma) = 1 - \frac{\sigma}{\sigma_f} \quad si \quad -\sigma_f \leq \sigma < 0 \quad (25)$$

$$F(\sigma) = 0 \quad si \quad \sigma < -\sigma_f \quad (26)$$

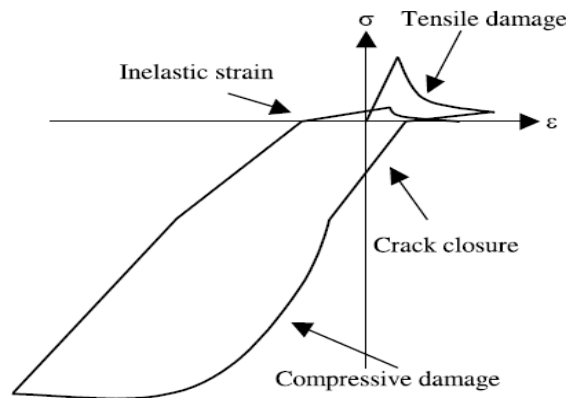


Fig. 2 Uniaxial response of the unilateral model

If the shearing strain is not negligible the biaxial behaviour is reduced to the stresses σ_{xx} and σ_{yy} , for each layer of the beam (Timoshenko) element. The non-linear system to solve is written (Dubé 1994, Kotronis 2000):

$$\begin{pmatrix} \varepsilon_{xx} & \varepsilon_{xy} \\ \varepsilon_{yx} & \varepsilon_{yy} \end{pmatrix} = \left(\Lambda^{-1}(\sigma, D_1, D_2) \right) \begin{pmatrix} \sigma_{xx} & \sigma_{xy} \\ \sigma_{yx} & \sigma_{yy} \end{pmatrix} \quad (27)$$

$$\varepsilon_{xx} = \frac{\sigma_{xx}^+}{E_0(1-D_1)} + \frac{\sigma_{xx}^-}{E_0(1-D_2)} + \frac{\beta_1 D_1}{E_0(1-D_1)} \frac{\partial f(\sigma)}{\partial \sigma} + \frac{\beta_2 D_2}{E_0(1-D_2)} \quad (28)$$

$$\varepsilon_{xy} = \frac{\sigma_{xy}^+}{E_0(1-D_1)} + \frac{\sigma_{xy}^-}{E_0(1-D_2)} + \frac{\nu \sigma_{xy}}{E_0} \quad (29)$$

4. The behaviour of steel

In order to describe the non-linear behaviour of reinforcement, one chooses the classical plasticity model which take into account the non-linear kinematic hardening (Fig. 3) is used.

The free potential energy for this model is expressed as follows (Kotronis 2000, Kotronis 2005 and al, Davenne et al. 2003):

$$\rho \psi = \frac{1}{2} (\varepsilon - \varepsilon_p) : C : (\varepsilon - \varepsilon_p) + \frac{1}{2} b \alpha : \alpha \quad (30)$$

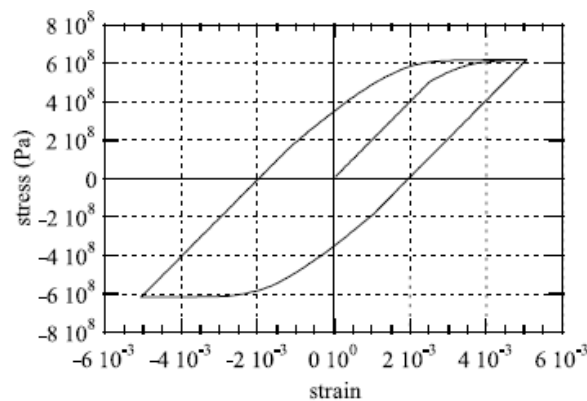


Fig. 3 Cyclic response of the plasticity steel model

With C is the elasticity tensor and α an internal variable associated with the kinematic hardening. The constitutive laws defined by derivation of this energy give:

$$\sigma = \frac{\partial \rho \psi}{\partial \varepsilon} = C : (\varepsilon - \varepsilon_p) \quad (31)$$

$$X = \frac{\partial \rho \psi}{\partial \alpha} = b \alpha \quad (32)$$

where X is the stress-like hardening variable.

The threshold function of the model has the form:

$$f = J_2(\sigma - X) + \frac{3}{4} d X : X - \sigma_y \quad (33)$$

where b, d and σ_y are the model parameters to identify.

The reinforcement has a privileged orientation and the uniaxial law is sufficient to reproduce its behaviour (Kotronis 2000). The reinforcement can be considered as concentrate or diffuse in the concrete elements. In the first case, elements bars with non-linear behaviour, whose position and section coincide with the position and section of real reinforcement, are used. In the second case the behaviour of the mixed layers (Fig. 1) is homogenized by a law of mixtures to calculate the stress layer in proportion to each material (The adherence steel-concrete is supposed perfect; i.e, identical strain on the two materials at their frontier). Thus, in each layer (Mazars 2001):

$$\varepsilon_{concrete} = \varepsilon_{steel} \quad (34)$$

$$E = (1 - C_{a/b}) \times E_{concrete} + C_{a/b} \times E_{steel} \quad (35)$$

$$\varepsilon_{an} = (1 - C_{a/b}) \times \varepsilon_{an.concrete} + C_{a/b} \times \varepsilon_{an.steel} \quad (36)$$

$$C_{a/b} = \frac{A}{B} \quad (37)$$

where: E : is the homogenized Young modulus (steel + concrete).

$C_{a/b}$: is the ratio surface of reinforcement.

A : is the relative steel air within the reinforced layer.

B : is the relative concrete air within the reinforced layer.

$\varepsilon_{an.concrete}$: is the anelastic concrete stain.

$\varepsilon_{an.steel}$: is the anelastic steel stain; and

ε_{an} : is the anelastic strain homogenized of the reinforced layer (steel + concrete).

5. Applications

5.1 Modelling of a reinforced concrete beam (Benchmark MECA(Ghavamian 2001))

In order to highlight the results which can be obtained with the multi-layered elements

modelling , the MECA benchmark will be used. Considering a beam of a rectangular section in concrete reinforced by steels (Fig. 4), subjected to a 3 points bending with a static loading of increasing intensity applied to the beam medium. The same example was studied by Ragueneau (2006).

The MECA beam is characterized by its twinge, it behaves as bending beam. The influence of shearing is negligible and the multi-layered beam of Bernoulli kinematics modelling, with uniaxial laws behaviour for the concrete and steel, is sufficient (Kotronis 2000).

The concrete behaviour follows the damage Laborderie model (unilateral law behaviour). The concrete characteristics are represented in the table 1.

The steel behaviour is supposed elastoplastic with kinematic hardening with a Young's modulus of 200000 MPa and an elastic limit equal to 400 MPa.

Fig. 5 shows the numerical model (2D) of MECA beam, carried out by the present modelling. The beam is modelled by 10 beam elements with 2 nodes and 2 integration points, the section of each element is discretized by 10 superimposed layers, including 8 out of concrete alone and 2 simultaneously including concrete and steel.

Fig. 6 shows a comparison of the load-deflection response between the present numerical simulation and the experimental and numerical results of Ragueneau (2006).

The present model can be compared to the references modes, i.e, Ragueneau (2006) and the experimental model.

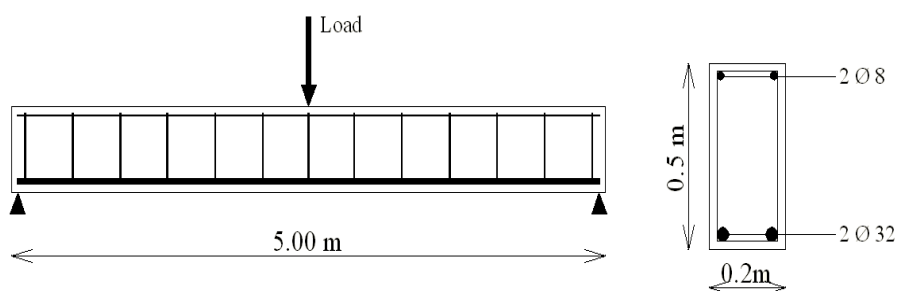


Fig. 4 Reinforced concrete beam of MECA benchmark

Table 1 Concrete characteristics for this model (Moulin.2012)

Young's modulus	37272 e ⁶ Pa
Density	2400 kg/m ³
Damage threshold in tension	310 Pa
Damage threshold in compression	7000 Pa
Damage threshold in compression	9e-3 Pa ⁻¹
Damage parameter in compression	5.30e ⁻⁶ Pa ⁻¹
Parameter for tension	1.20
Parameter for compression	2.00
Permanent strain activation in tension	1.00e ⁶ Pa
Permanent strain activation in compression	-40e ⁶ Pa
Crack closure stress	3.50e ⁶ Pa

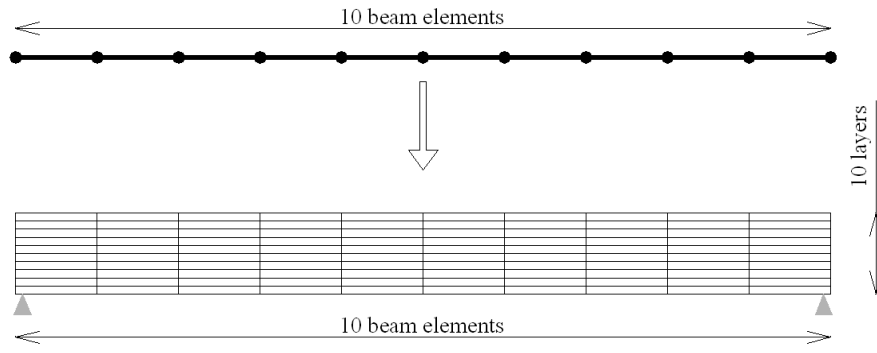


Fig. 5 MECA beam Discretization in multi-layered element

Fig. 6 Load-displacement curve of MECA beam

The first part of the load-displacement curve established by the present modelling, is linear until a force of 45000 N. this force is reached for a displacement of 2.04 mm. The beam stiffness is then of $45000/0.00204 = 22080471.1\text{N/m}$. The end of the linear phase indicates the apparition of the bending first crack. In the second part of the curve, the concrete is in the non-linear field but the reinforcements did not yet plasticize. Every change of the slope corresponds to a crack therefore a redistribution of the efforts in the beam. The steel plasticizations occur for a displacement of 0 .01719 m, corresponding to a load of 220000 N.

Figs. 7, 8 and 9 progressively show the damage cards due to tension during the loading. The first state damage to appear for a displacement of 0.001431m Fig. 7), it is localized in the beam mid-span. This damage is developed along the lower part of the beam (Fig. 9).

Another beam was modelled with an imposed displacement applied at mid-span (Fig. 10). The beam is modelled by 16 beams elements with 2 nodes and 2 integrations points, the section of each element is discretized by 20 superimposed layers, of which 18 in concrete alone and 2 simultaneously including concrete and steel (Fig. 11). A comparison between the present results and those of Moulin (2012) obtained by the Aster's code was established.

The concrete behaviour follows the damage Laborderie model (unilateral law behavior). The concrete characteristics are represented in table 1.

This beam has the same concrete and steel characteristics as the previous case.

The evolution of the support reaction terms of the mid-span displacement of the beam is shown in Fig. 12. In comparison with the results of Moulin (2012) model, there is a very good agreement between the two results.

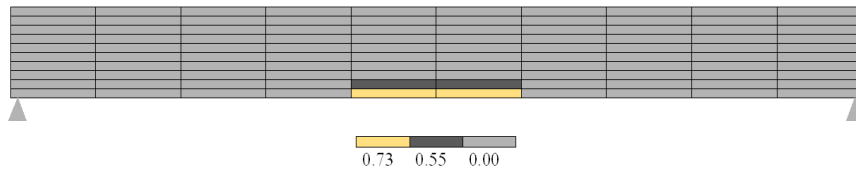


Fig. 7 Damage chart in tension $\langle D_1 \rangle$ for 0.001431m deflection

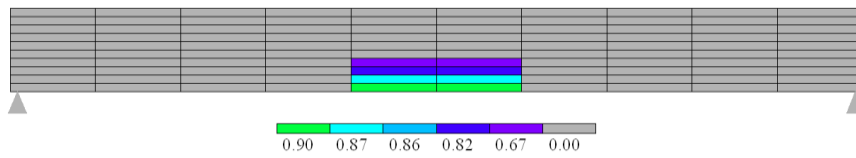


Fig. 8 Damage chart in tension $\langle D_1 \rangle$ for 0.00204m deflection

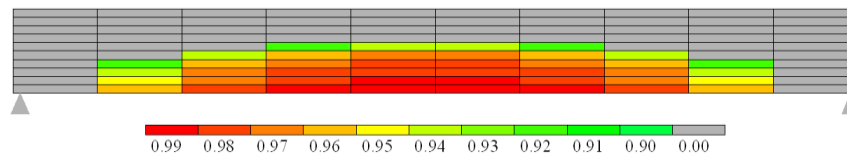


Fig. 9 Damage chart in tension $\langle D_1 \rangle$ for 0.01719m deflection

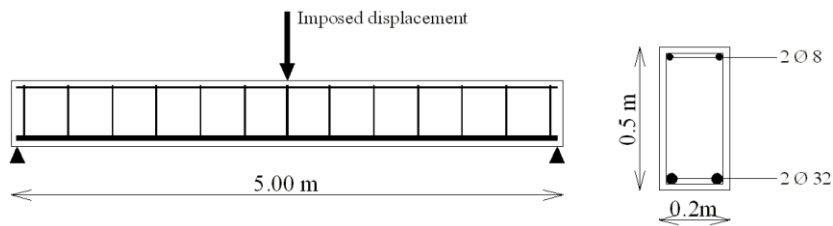


Fig. 10 reinforced concrete beam of MECA benchmark

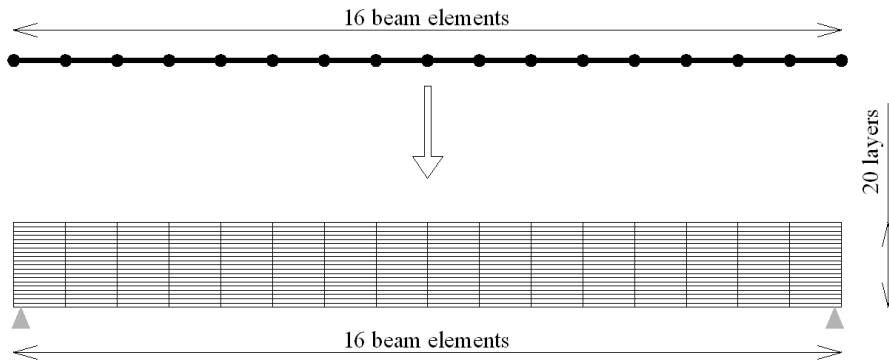


Fig. 11 Numerical model beam

Fig. 12 Support reaction, as a function of the displacement at the mid-span of the beam

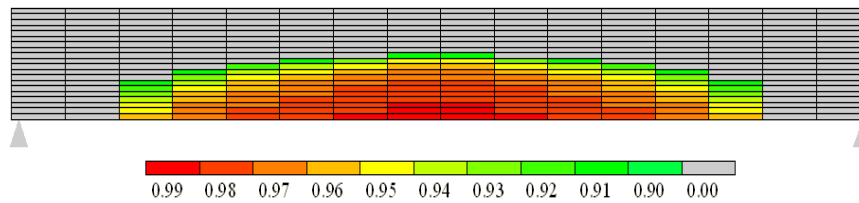


Fig. 13 damage chart in tension «D₁»

The damage chart in tension at the end of the loading is shown in Fig. 13. The damage indicator varies between 0 and 1. By filtering these values between 0.9 and 1, we remove the micro-cracks in order to obtain an image of the macro-cracks. The beam is mainly damaged in the lower part.

5.2 Column buckling

The purpose of this example is to perform a modelling of a reinforced concrete column with rectangular section subjected to an axial loading with an eccentricity $e = 1.5\text{cm}$ (Fig. 14(a)). The same column was studied experimentally by Fouré (1978) and numerically discretization by Franz (1994) with multi-fiber elements (Willam-Warnke behaviour law).

In this paper, the column is modeled by 11 multi-layered elements with 2 nodes and 2 integration points. The section of each element is discretized by 06 superimposed layers, of which 4 in concrete alone and 2 in concrete and steel (Fig. 14(b)). The eccentric axial load is modelled by a centered axial load F and a bending moment $M = F \times e$. The weight of the column is neglected.

The concrete behaviour obeyed the Laborderie damage model (unilateral law behaviour). The characteristics considered for the concrete are shown on table 2.

The steel behaviour is supposed elastoplastic with kinematic hardening. The steels characteristics used are:

Young modulus: 200000 MPa;

Elastic limit: 400 MPa.

Fig. 15, shows the load variation according to the horizontal displacement of the top of the column. This figure gives a comparison between the results obtained by the present modelling, the experimental results of Fouré (1978) and those obtained by Franz (1994). As it can be seen from Fig. 15, there is a good agreement between these models.

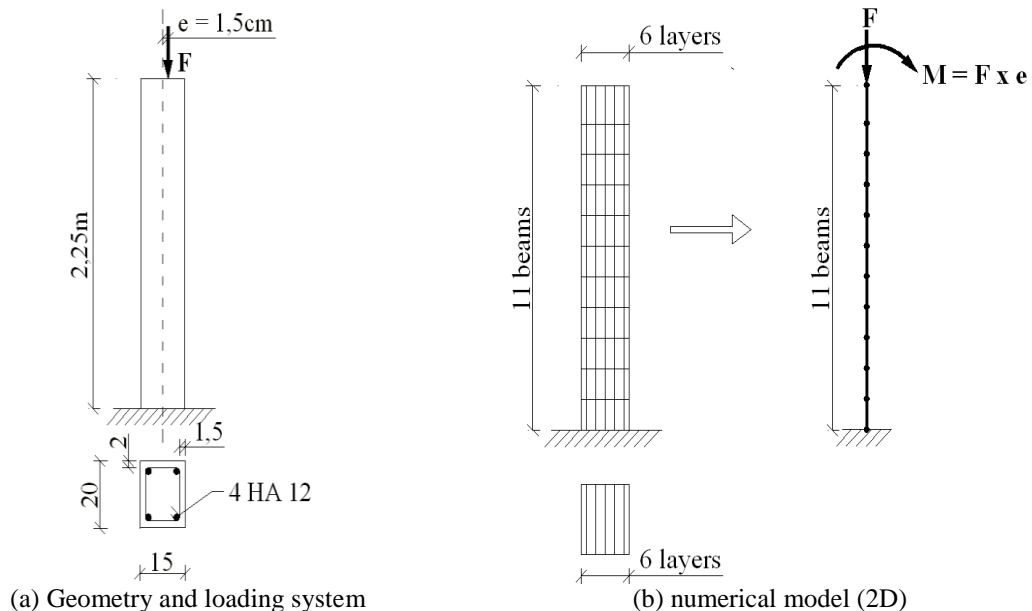


Fig. 14 Geometry and 2D numerical model of Fouré Column

Table 2 Concrete characteristics for Laborderie model

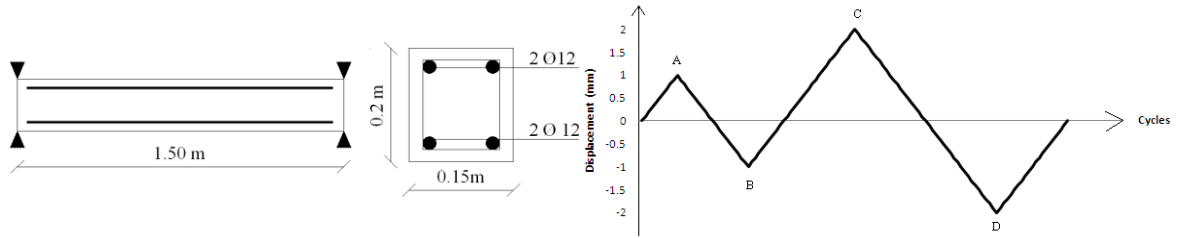
Young's modulus	30000 e ⁶ Pa
Density	2500 kg/m ³
Damage threshold in tension	220 Pa
Damage threshold in compression	9000 Pa
Damage threshold in compression	9e ⁻³ Pa ⁻¹
Damage parameter in compression	5.30e ⁻⁶ Pa ⁻¹
Parameter for tension	1.20
Parameter for compression	1.40
Permanent strain activation in tension	1.00e ⁶ Pa
Permanent strain activation in compression	-40e ⁶ Pa
Crack closure stress	1.30e ⁶ Pa

Fig. 15 Load-displacement of the top column

5.3 Cyclic response modelling of a reinforced concrete beam

This example is used to validate the cyclic bending behaviour of a reinforced concrete beam (Fig. 16(a)). The loading is composed of an amplitude cycle of 1mm followed by an amplitude cycle of 2 mm (Fig. 16(b)).

The model used in this paper is a structure of 20 beams elements with 2 nodes and 2



(a) Geometry and reinforcement beam

(b) The loading history

Fig. 16 Geometry and numerical model (2D)

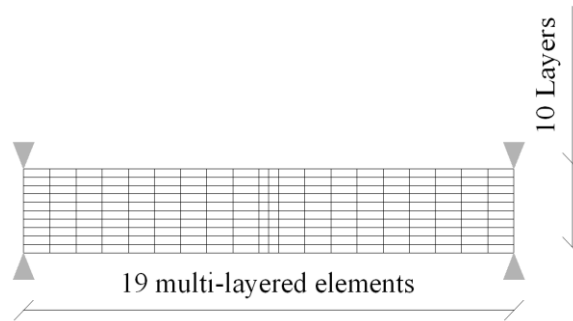


Fig. 17 Beam discretisation in multi-layered elements

Fig. 18 Load-displacement response for different models

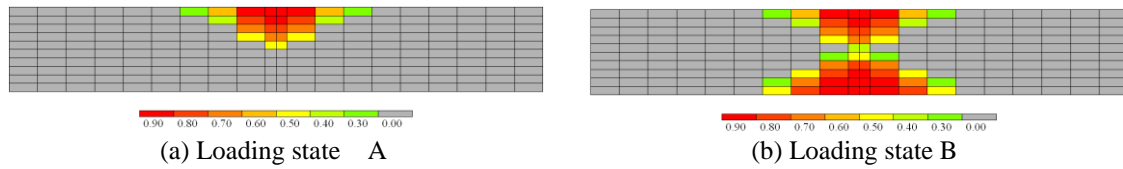


Fig. 19 Damage chart in tension «D1 » for the first cyclic loading

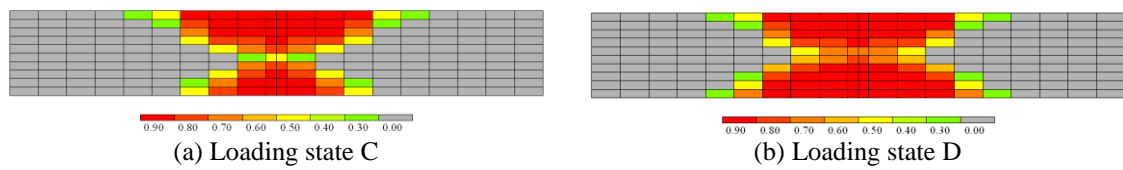


Fig. 20 Damage chart in tension «D1 » for the second cyclic loading

integrations points. The section of each element is discretized by 10 superimposed layers, including 8 out of concrete alone and 2 simultaneously including concrete and steel (Fig. 17).

The same concrete and steel behaviour as the previous examples are used in this case.

The cyclic response of the beam shown on the Fig. 18, are compared with the test results. As it can be seen from this figure, a very good coherence between the two results.

This figure shows also presents a comparison of the load-displacement response obtained by the present simulation (modeling by multi-layered elements with a Laborderie law) and that obtained by Matallah (2009). The two numerical models gave similar results in first cyclic loading. However, for the second cyclic loading, a light differences are observed.

Fig. 19 presents the damage chart of the beam for the first cyclic loading. In the loading state « A » the higher part of the beam is damaged (Fig. 19(a)). The loading state « B » corresponds to an opposed loading, the damage state initially product is always stored whereas a new damage state is created in the lower part of the beam (Fig. 19(b)).

The damage chart of the beam during the second cyclic loading is shown in Fig. 20.

6. Conclusions

A simple modelling of the non-linear behaviour of the reinforced concrete structure is presented. It uses a multi-layered beams elements which obeyed the Bernoulli hypothesis to confer to the various layers an uniaxial behaviour. It also allows the description of the structures damage state during a loading.

Four examples of applications were presented. The first one is a beam subjected to a 3 points flexion with static loading of increasing intensity applied to the mid-span of the beam (MECA Benchmark), the second one was a beam subjected to 3 points flexion with an imposed displacement at mid-span of the beam. The third, is a column buckling test (Fouré column) and the fourth of a beam in cyclic bending. According to these examples it was noticed:

- A very good coherence between the present numerical results and the experimentation results.
- A good concordance between the results of present numerical models and those of other numerical models of references.

- The non-linear analysis reflects the real behavior of reinforced concrete structures.
- If the material is discharged after having undergone a damage state, it restores its stiffness, the crack previously open are closed again but the internal structure of material remains always damaged.

References

Davenne, F., Ragueneau, F and Mazars, J. and Ibrahimbegovic, A. (2003), “Efficient approaches to finite element analysis in earthquake engineering”, *Comput. Struct.*, **81**, 1223-1239.

Kotronis, P., Ragueneau, F and Mazars, J. (2005), “A simplified modelling strategy for R/C walls satisfying PS92 and EC8design”, *Eng. Struct.*, **27**, 1197-1208.

Matallah, M. and Laborderie, C.(2009), “Inelasticity–damage-based model for numerical modeling of concrete cracking”, *Eng. Fract. Mech.*, **76**, 1087-1108.

Matallah, M. and Laborderie, C.(2007), “Modélisation numérique de l’ouverture des fissures dans les structures en béton”, *25^e rencontres de l’AUGC*, Bordeaux, France, Mai.

Mazars, J., Ragueneau, F. and Kotronis, P. (2001), “ La simulation numérique, la simulation physique, 2 approches complémentaires pour l’analyse des effets des risques naturels : le cas des séismes”, *XV^{ème} congrès français de mécanique*, Nancy, France, Septembre.

Franz-Josef, ULM. (1994), “Modélisation elastoplastique avec endommagement du béton de structures. Application aux calculs statiques et dynamiques de structures en béton arme et béton précontraint”, Thèse de doctorat, Ecole Nationale des ponts et Chaussées, Paris.

Kotronis, P. (2000), “ cisaillement dynamique de murs en béton armé. Modèles simplifiés 2D et 3D”, Thèse de Doctorat, Ecole normale supérieure de Cachan, Cachan.

Laborderie, C. (2003), “ Stratégies et Modèles de Calculs pour les Structures en Béton”, Thèse d’habilitation à diriger les recherches, Université de Pau et des Pays de l’Adour.

Ragueneau, F. (1999), “Fonctionnement dynamique des structures en béton – Influence des comportements hystérétiques locaux”, Thèse de doctorat, Ecole normale supérieure de Cachan, Cachan.

Ragueneau, F. (2006), “Comportements endommageants des matériaux et des structures en béton armé”, Mémoire d’habilitation à diriger des recherches, Université Pierre et Marie Curie , Paris 6.

Fouré, B. et Virlogeux, M. (1978), “ le flambement des poteaux compte tenu du fluage du béton”, *Annls. De l’I.T.B.T.P.*, n° 359, Mars.

Stéphane, M. (2012), “Réponse statique d’une poutre en béton armé (section rectangulaire) à comportement non linéaire”, *Manuel de validation, Code_Aster*, fascicule V6. Août

Stéphane, M. (2012), “Réponse sismique d’une poutre en béton armé (section rectangulaire) à comportement non linéaire”, *Manuel de validation, Code_Aster*, fascicule V5.02, Août

Ghavamian, S. (2001), “MECA project benchmark: Three dimensional non linear constitutive models of fractured concrete. Evaluation-Comparison-Adaptation”, Edited by EDF R&D.